
Flight and Static Exhaust Flow Properties of an F110-GE-129 Engine in an F-16XL Airplane During Acoustic Tests

Jon K. Holzman, Lannie D. Webb, and Frank W. Burcham, Jr.
NASA Dryden Flight Research Center
Edwards, California

1996



National Aeronautics and
Space Administration

Dryden Flight Research Center
Edwards, California 93523-0273

CONTENTS

| | <u>Page</u> |
|---|-------------|
| ABSTRACT | 1 |
| NOMENCLATURE | 1 |
| INTRODUCTION | 2 |
| F-16XL AIRCRAFT DESCRIPTION | 3 |
| Inlet Description | 3 |
| Engine Description | 6 |
| MEASUREMENTS | 6 |
| Aircraft | 6 |
| Engine | 7 |
| Acoustics Measurements | 7 |
| Flyover Tests | 7 |
| Flyover Space Positioning | 8 |
| Static Acoustic Tests | 8 |
| Meteorology | 9 |
| TEST PROCEDURES | 9 |
| Climb-To-Cruise Tests | 10 |
| ANOPP Tests | 10 |
| Static Tests | 11 |
| ANALYTICAL TECHNIQUES | 11 |
| Engine Exhaust Flow Properties | 11 |
| F110-GE-129 Digital Engine Model | 12 |
| Engine Model Description | 12 |
| Data Selection Procedure | 12 |
| Engine Model Inputs | 12 |
| Engine Model Output | 14 |
| Exhaust Flow Properties | 14 |
| Ideal or <i>Jet</i> Expansion Parameters | 14 |
| Area Ratio Parameters | 14 |
| Exhaust Static Temperature | 14 |
| Local Speed of Sound and Exhaust Velocities | 15 |
| RESULTS AND DISCUSSION | 15 |
| Verification of F110-GE-129 Engine Deck | 19 |
| Ground Static Test Results | 23 |

| | |
|---|----|
| Flyover Exhaust Flow Properties Results | 23 |
| CTC Test Results | 23 |
| ANOPP Test Results | 24 |
| CONCLUDING REMARKS | 25 |
| REFERENCES | 26 |

TABLES

| | |
|--|----|
| 1. Climb-to-cruise test points | 10 |
| 2. ANOPP test points | 10 |
| 3. Acoustics flight tests for the F-16XL, ship 2 | 11 |
| 4. F-16XL, ship 2, ground run test | 15 |
| 5. CTC test data | 17 |
| 6. ANOPP flyover test data. | 18 |

FIGURES

| | |
|--|----|
| 1. The F-16XL, ship 2, airplane | 4 |
| 2. The F-16XL, ship 2, inlet (893 in ² capture area) | 5 |
| 3. Cutaway view of the F110-GE-129 engine and station designations | 6 |
| 4. Ground track and array layout on Rogers Dry Lake, Edwards, CA | 7 |
| 5. Microphone array for the F-16XL, ship 2, ground static acoustic survey | 8 |
| 6. Photograph of the F-16XL, ship 2, ground acoustic test showing 3 microphones in foreground | 9 |
| 7. Ambient temperature and standard day temperature for the acoustics flyover tests | 13 |
| 8. Comparison of measured and deck-calculated parameters, ground run | 20 |
| 9. Comparison of measured and deck-calculated parameters, climb-to-cruise tests | 21 |
| 10. Comparison of measured and deck-calculated parameters, ANOPP tests | 22 |
| 11. Exhaust flow properties, F110-GE-129 engine in F-16XL, ship 2, ground run | 23 |
| 12. Exhaust flow properties, F110-GE-129 engine in F-16XL, ship 2, climb-to-cruise tests, all tests at intermediate power, for altitudes, see table 5 | 24 |
| 13. Exhaust flow properties, F110-GE-129 engine in F-16XL, ship 2, ANOPP tests, 3800 ft altitude | 25 |

ABSTRACT

The exhaust flow properties (mass flow, pressure, temperature, velocity, and Mach number) of the F110-GE-129 engine in an F-16XL airplane were determined from a series of flight tests flown at NASA Dryden Flight Research Center, Edwards, California. These tests were performed in conjunction with NASA Langley Research Center, Hampton, Virginia (LaRC) as part of a study to investigate the acoustic characteristics of jet engines operating at high nozzle pressure conditions. The range of interest for both objectives was from Mach 0.3 to Mach 0.9. NASA Dryden flew the airplane and acquired and analyzed the engine data to determine the exhaust characteristics. NASA Langley collected the flyover acoustic measurements and correlated these results with their current predictive codes. This paper describes the airplane, tests, and methods used to determine the exhaust flow properties and presents the exhaust flow properties. No acoustics results are presented.

NOMENCLATURE

| | |
|------------|---|
| A_8 | exhaust nozzle physical area at the throat, in ² |
| A_9 | exhaust nozzle physical area at the exit plane, in ² |
| AE_8 | exhaust nozzle effective throat area, in ² |
| AE_9 | exhaust nozzle effective exit-plane area, in ² |
| AFFTC | Air Force Flight Test Center, Edwards AFB, California |
| AGL | above ground level |
| ANOPP | Aircraft Noise Prediction Program |
| CTC | climb to cruise |
| EGT | exhaust gas temperature downstream of the turbine, °R |
| F_g | gross thrust, lbf |
| GAM7 | specific heat ratio of exhaust gas at nozzle entrance |
| <i>jet</i> | location where exhaust flow has expanded to ambient pressure |
| M_9 | nozzle exit Mach number based on nozzle expansion ratio |
| M_{jet} | fully expanded <i>jet</i> Mach number |
| Mach | Mach number |
| Meas | measured |
| NPR | nozzle pressure ratio (P_8/P_{amb}) |
| N_1 | fan rotor speed, rpm |
| N_2 | core rotor speed, rpm |
| OH | overhead |
| P_1 | engine face total pressure, lbf/in ² |
| P_{s3} | compressor discharge static pressure, lbf/in ² |
| $PT_{2.5}$ | fan discharge total pressure, lbf/in ² |

| | |
|------------|---|
| $P7$ | exhaust nozzle entrance total pressure, lbf/in ² |
| $P8$ | exhaust nozzle throat total pressure, lbf/in ² |
| P_{amb} | ambient static pressure, lbf/in ² |
| PLA | power lever angle, deg |
| PLF | power for level flight |
| P_{s9} | exit plane static pressure, lbf/in ² |
| T_{amb} | ambient temperature, deg |
| $T1$ | engine face total temperature, °R |
| $T8$ | exhaust-nozzle mixed <i>jet</i> total temperature at the throat, °R |
| T_{s9} | exhaust nozzle exit static temperature, °R |
| T_{sjet} | fully expanded <i>jet</i> static temperature, °R |
| $V9$ | velocity at nozzle exit, from $M9$, ft/sec |
| V_{jet} | fully expanded nozzle <i>jet</i> velocity, ft/sec |
| WFE | core engine fuel flow, lb/h |
| $W8$ | mass flow rate at the exhaust nozzle throat, lb/sec |

INTRODUCTION

Exhaust flow properties (mass flow, temperature, pressure, velocity, and Mach number) of an engine are key in determining the acoustic characteristics. Airport noise is one of the key issues in determining the environmental acceptability of proposed supersonic transport airplanes. These airplanes will probably be powered by engines operating at high nozzle pressure ratios (NPR) and high exhaust *jet* velocities. Concern exists not only for noise produced during takeoff and landing but also for noise produced along the flightpath of the airplane during the subsonic portion of the climb out for a distance of up to 50 miles.

To determine the engine noise for these transport designs, acoustic codes, such as the Aircraft Noise Prediction Program (ANOPP), are used.¹ These codes were developed and validated using data acquired from engines with NPR's and flight speeds lower than that planned for supersonic transports. Doppler amplification of the shock noise in the forward approach arc of the vehicle flightpath was of particular concern.

For these reasons, NASA Langley Research Center, Hampton, Virginia (LaRC), and Dryden Flight Research Center, Edwards, California, jointly conducted tests to acquire in-flight acoustic data for high NPR engines. Results of these tests would be used to update and validate the current noise predictive codes. The two main flight test objectives were to assess subsonic climb-to-cruise (CTC) noise using an aircraft with high NPR engines and to obtain an improved noise database to validate the ANOPP and other noise predictive codes. The test airplanes included an F-18 powered by two F404-GE-400 engines, (General Electric Company, Lynn, Massachusetts) and an F-16XL, ship 2, powered by a single F110-GE-129 engine (General Electric Company, Evendale, Ohio). The F-18 exhaust characteristics were presented in reference 2. NASA Dryden responsibilities for the F-18 airplane are discussed in reference 3. For the F-16XL, ship 2 tests, the responsibilities were to plan and conduct the flyover tests, record and analyze the

flight data, determine the airplane space position, determine the engine exhaust gas flow properties, and conduct a ground static acoustic survey. NASA Langley responsibilities were to setup the microphone array, record the noise measurements, merge the acoustic and space position data, analyze and evaluate the acoustic data, and correlate these data with Dryden-determined engine exhaust properties. The preliminary acoustic results are presented in the footnoted report.*

The F-16XL, ship 2, study consisted of flights over a microphone array at varying speeds and altitudes. Two types of flight tests were conducted: subsonic CTC noise determination and ANOPP predictive code validation. In the subsonic CTC portion of the study, flyovers were conducted at altitudes from 3,800 to 12,300 ft and from Mach 0.3 to Mach 0.95 all at an intermediate (maximum nonafterburning) power setting. For the ANOPP evaluation flyovers, the tests were flown at 3,800 ft and from Mach 0.3 to Mach 0.95. A static ground-level engine-run test was also conducted over the power setting range from idle to intermediate power in order to establish baseline exhaust acoustic noise levels with no forward airplane velocity.

This paper describes the F-16XL airplane and F110-GE-129 engine, presents the flight tests performed using the F-16XL airplane, documents the test and analysis techniques used to calculate the engine flow properties, and presents the engine exhaust flow properties. Acoustics data are not presented. Use of trade names or names of manufacturers in this document does not constitute an official endorsement of such products or manufacturers, either expressed or implied, by the National Aeronautics and Space Administration.

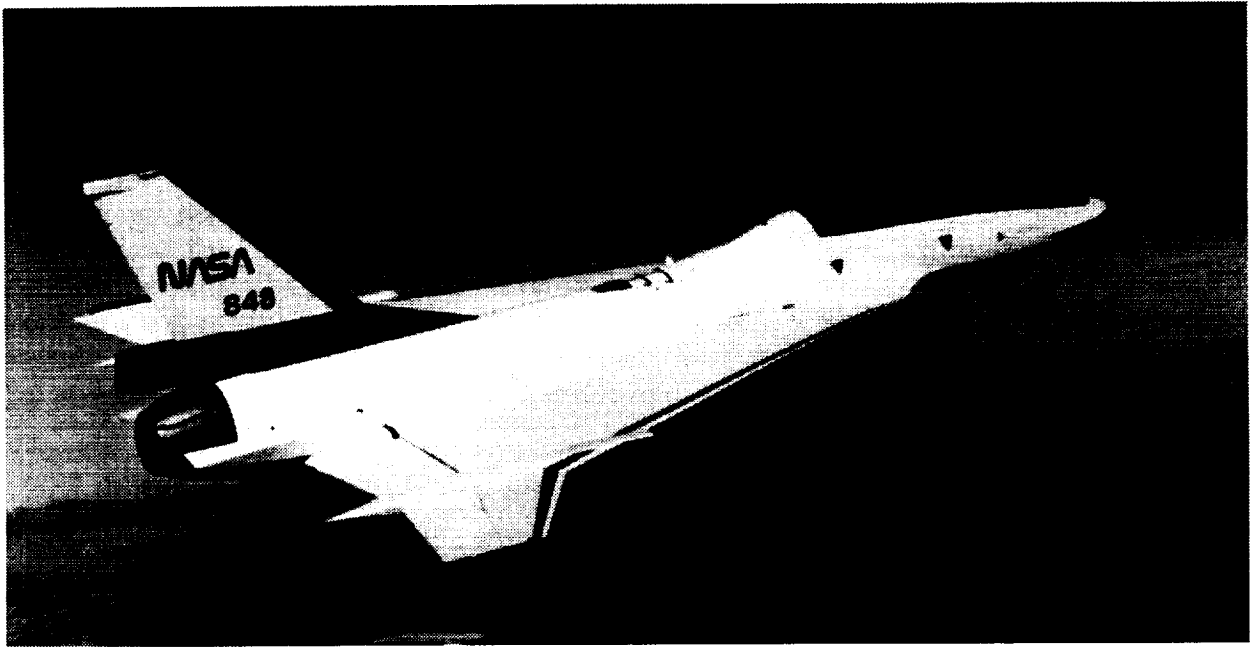
F-16XL AIRCRAFT DESCRIPTION

The F-16XL airplane has a "cranked" delta wing and is an extensive modification of the F-16 airplane (fig. 1). Two aircraft were built by Lockheed-Martin (formerly General Dynamics, Fort Worth, Texas). The F-16XL, ship 2, a two-seat aircraft, has a length of 54.2 ft, a wingspan of 34.3 ft, and a maximum weight of approximately 36,000 lb. Figure 1(a) shows an in-flight photograph and figure 1(b) shows a three-view drawing with key dimensions of this airplane. It has a maximum Mach number of approximately 2.05 and a nominal design load factor of 9 g which provides a large performance envelope for flight research. The F-16XL, ship 2, aircraft is powered by a single F110-GE-129 afterburning turbofan engine mounted in the rear fuselage.

Inlet Description

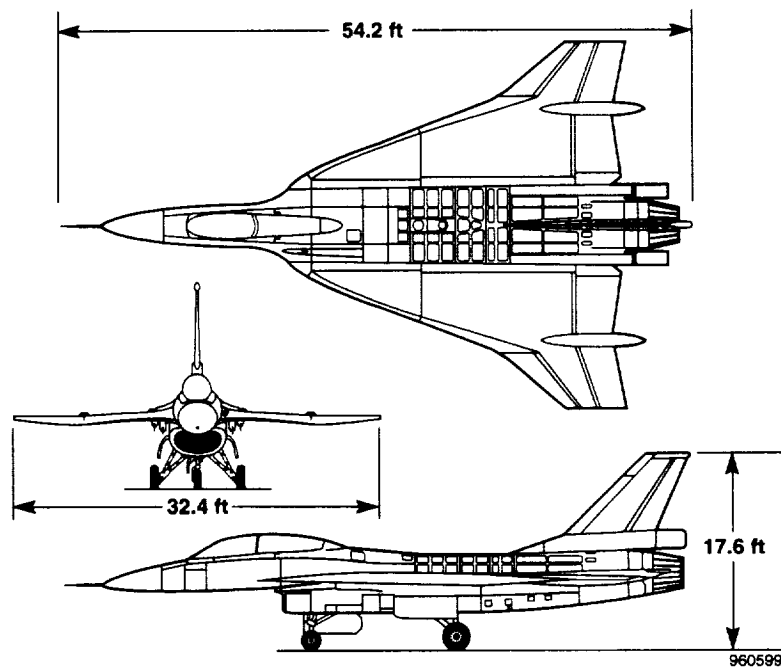
The F-16XL, ship 2, air inlet consists of a normal shock inlet mounted below the front fuselage followed by an S duct to the engine. Inlet size and pressure recovery characteristics are important in determining the engine exhaust flow conditions. A front view of the inlet is shown in figure 2(a). The inlet has a geometric capture area of 893 in². This area is 56 in² larger than the F-16 A/B small inlet but slightly smaller than the F-16 C/D big inlet. Figure 2(b) shows the total pressure recovery of this inlet, as determined from wind-tunnel tests, for a range of engine-corrected airflows and Mach numbers.

*Jeffrey J. Kelly, Mark R. Wilson, John Rawls Jr., Thomas D. Norum, and Robert A. Golub, *F-16XL and F-18 High Speed Acoustic Flight Test Data Base*, NASA CD TM-10006, 1996. (This is a controlled distribution document. Direct inquiries to the author of this document at NASA Langley Research Center Aeroacoustics Division.)



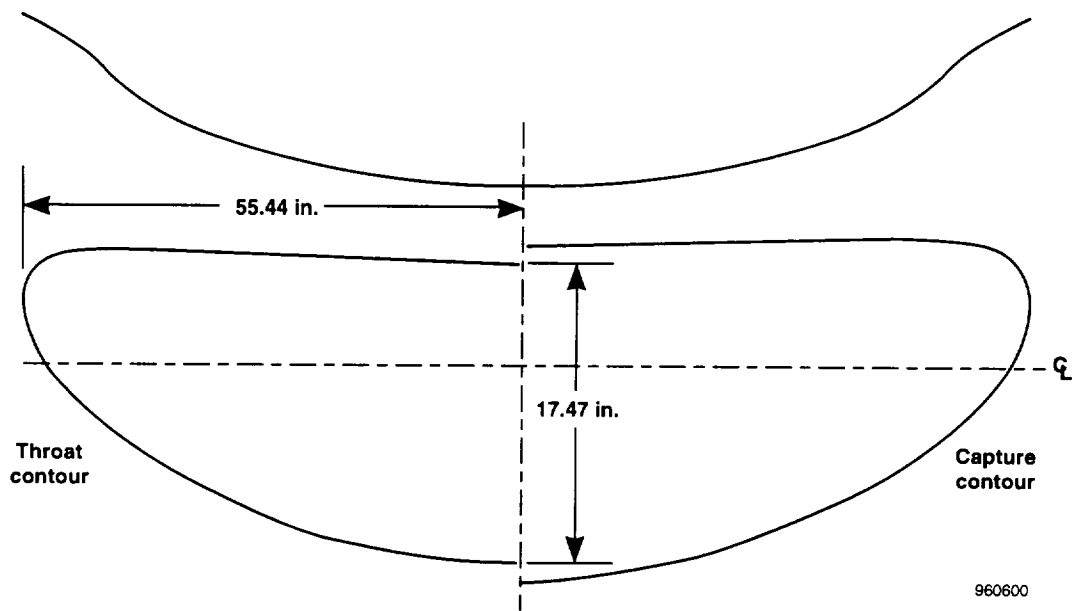
EC-91-646-1

(a) In-flight photograph.

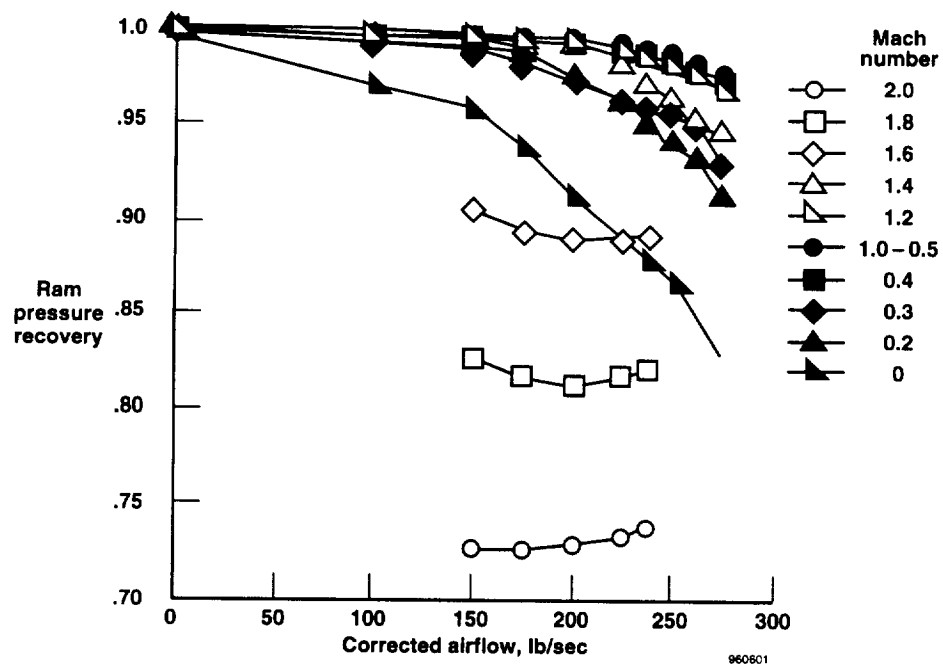


(b) Three-view drawing.

Figure 1. The F-16XL, ship 2, airplane.



(a) Drawing of the inlet capture area and throat area.



(b) Inlet ram pressure recovery.

Figure 2. The F-16XL, ship 2, inlet (893 in² capture area).

Engine Description

For the acoustic tests, the F-16XL, ship 2, was powered by the F110-GE-129 increased performance engine. This two-spool, low-bypass, axial-flow turbofan engine with afterburner has a maximum thrust of 29,000 lbf. Figure 3 shows a cut away schematic view of the engine depicting the station designations, including the “jet” station where the engine exhaust flow has adjusted to free stream static pressure. The engine features a three-stage fan driven by a two-stage, low-pressure turbine and a seven-stage, high-pressure compressor driven by a single-stage, high-pressure turbine. Variable inlet guide vane geometry is incorporated into the fan and the first four stages of the high-pressure compressor. A fan/core mixer is just upstream of the afterburner. The exhaust nozzle is of the convergent-divergent type with a variable throat area. The engine is equipped with a digital engine control unit which controls the fuel flows, rotor speeds, variable geometry, pressures, and temperatures in the engine. Idle power is at 20° power lever angle (PLA) setting, and intermediate (maximum nonafterburning) power is at 85° PLA. At this latter setting, the engine produces NPR similar to those proposed for some versions of future supersonic transport engine designs.

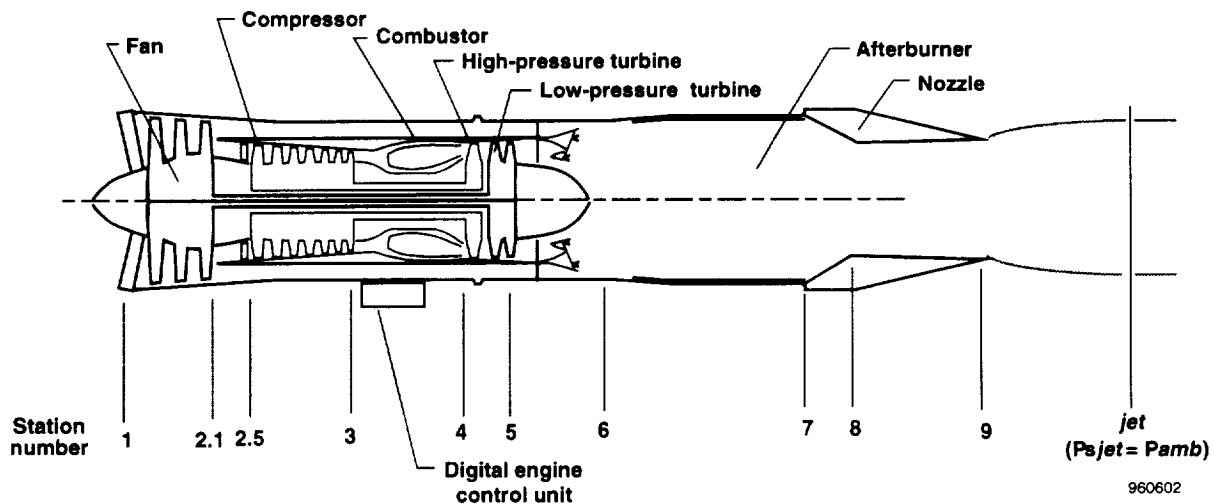


Figure 3. Cutaway view of the F110-GE-129 engine and station designations.

MEASUREMENTS

The F-16XL, ship 2, airplane was instrumented to measure parameters of interest for the acoustic fly-over test. Aircraft and engine parameters were included. In addition, acoustic, meteorological, and airplane space-positioning measurements were made on the ground.

Aircraft

The F-16XL, ship 2, Mach number and altitude were obtained from the pitot-static probe on the nose-boom. Pressures from the pitot probe were fed to the central airdata computer where Mach number and altitude were calculated. The aircraft also had an inertial navigation system for accurate velocity and position determination which was helpful in flying the airplane as close as possible to the designated

ground-track profile over the Edwards, California, fly-by line. Angle of attack and angle of sideslip were measured by vanes on the noseboom. These data were recorded at 10 samples/sec onboard on a 10-bit pulse code modulation (PCM) data system and were also transmitted to the ground. The airplane was equipped with a C-band radar beacon to aid in precise space positioning.

Engine

The F110-GE-129 engine was extensively instrumented. For this paper, the parameters of interest are those used as inputs to and for comparison with the F110-GE-129 engine deck and for the acoustic analysis. These parameters include PLA; engine face total temperature, $T1$; fan discharge total pressure, $PT2.5$; compressor discharge static pressure, $Ps3$; core engine fuel flow, WFE ; fan rotor speed, $N1$; core rotor speed, $N2$; engine exhaust gas temperature (EGT); and exhaust nozzle physical area at the throat, $A8$.

Acoustics Measurements

Flyover Tests

For the CTC and ANOPP tests, the acoustic data were measured with an analog and digital microphone array positioned along the flyby line on Rogers Dry Lakebed (fig. 4). This location provided a good proximity to the tracking radar, an adequate distance from the Edwards, California, main runway, and a large flat area suitable for acoustics measurements. The analog microphone setup was similar to the setup used by NASA Dryden during the static ground-run engine acoustic test.

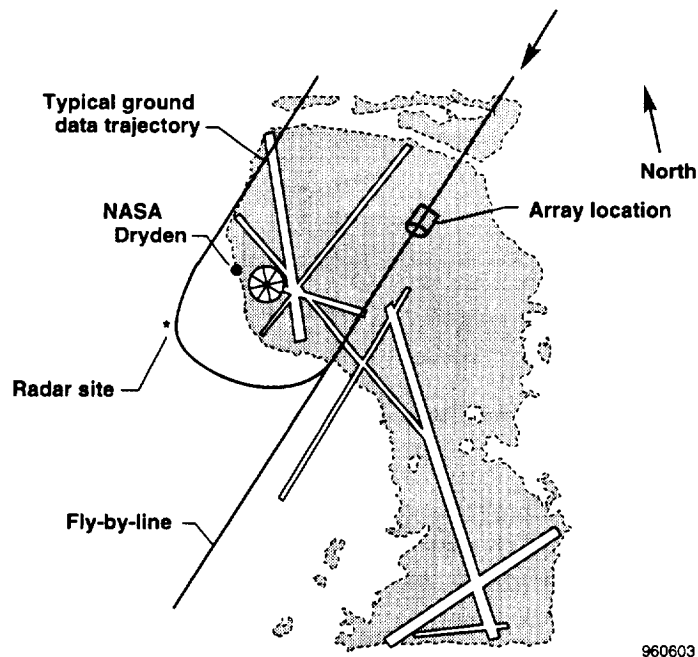


Figure 4. Ground track and array layout on Rogers Dry Lake, Edwards, CA.

Flyover Space Positioning

The NASA Dryden FPS-16 radar was used to track the radar beacon on F-16XL, ship 2, airplane during the acoustic flyovers. These data were used in the control room to assist the pilot in lineup, establish the time for beginning and completing data runs, and determine the validity of the track for each flyover. These data were also used by NASA Langley in the postflight analysis to determine the position of the airplane for correlation with the microphone data.

Static Acoustic Tests

For the static tests conducted by NASA Dryden, a 24-microphone array was located on a large flat taxiway area (fig. 5). Nominal microphone placement was every 7.5° on an arc 99 ft from the engine exhaust centerline. Inverted microphones were mounted inside windscreens with the diaphragms 0.5 in. above a thin aluminum plate which was taped to the concrete or asphalt surface. This setup allowed for measuring acoustic exhaust noise free of ground reflections.

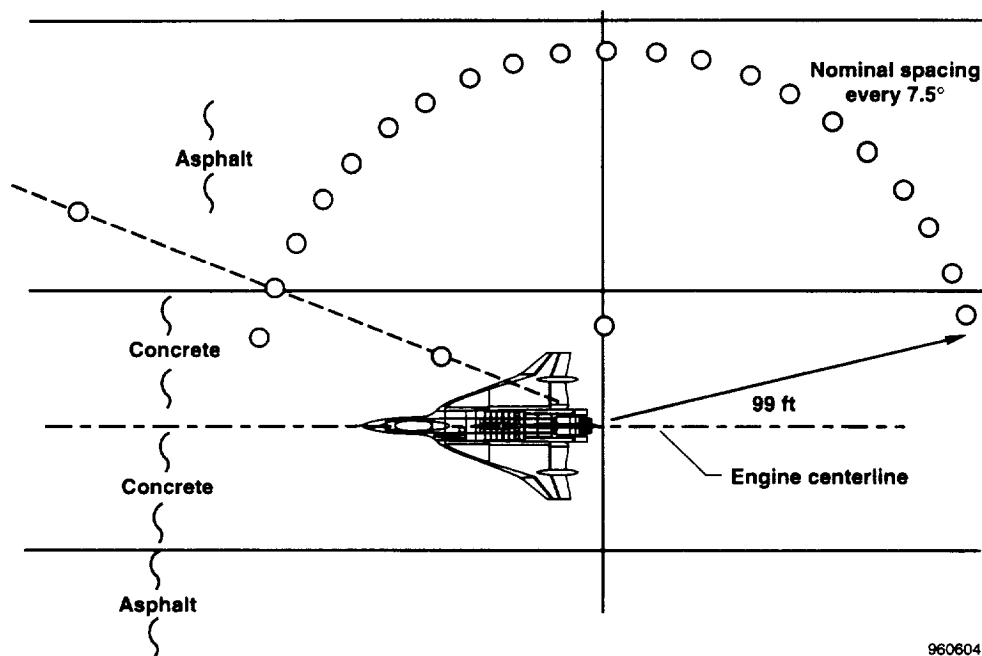


Figure 5. Microphone array for the F-16XL, ship 2, ground static acoustic survey.

Figure 6 shows the airplane positioned for the static test. Three of the microphones are visible. The NASA Dryden acoustics van was used to record the 24 channels of microphone data. Two 14-track tape recorders were installed in the mobile trailer. Twelve channels of acoustic data were recorded on each of the two recorders; meanwhile, the remaining two channels were used to record the time and the pilot's event marker. Each of the 24 microphone stations was battery powered and consisted of a condenser microphone, a preamplifier, and a line driver amplifier. Each station was connected to a separate line driver by 1000 ft of shielded, coaxial signal cable. The line driver signal was in turn connected to one of the recorder data channels in the trailer, using a 1000-ft length of neoprene-covered cable containing a shielded, twisted pair of copper signal wires. The trailer also contained a weather station for recording

local temperatures as well as wind velocity and direction in the area of the microphone array and radios for communication with the airplane.

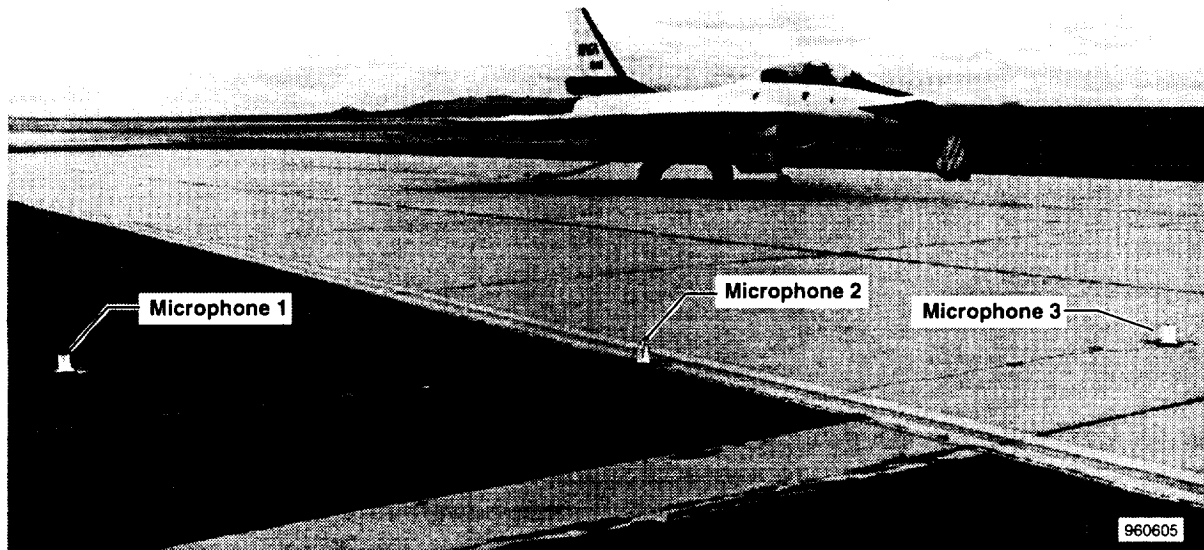


Figure 6. Photograph of the F-16XL, ship 2, ground acoustic test showing 3 microphones in foreground.

Meteorology

Atmospheric properties affect the propagation of acoustics and are one of the inputs into the ANOPP. Conditions for the flight data were determined from four sources:

1. The F-16XL, ship 2, onboard measurements
2. The weather balloons
3. A ground weather station at the acoustics van
4. A tethered balloon located near the flyover array

The onboard measurements were primarily winds aloft data readout from the airplane inertial system and *T1*. The tethered balloon was raised and lowered periodically during the tests using a 1500-ft tether.

TEST PROCEDURES

To satisfy dual objectives of the program, two flight tests were conducted: subsonic CTC noise determination and ANOPP predictive code validation. In both cases, obtaining acoustic data during the period when the airplane was more than 10° to 15° above the horizon as measured from the center of the acoustic array was desired. Distances of the start and end points away from the acoustic array were, therefore, a function of the test altitude. At the lowest test altitude, 1500 ft above ground level (AGL), this distance was approximately 1 mile. The pilot flew along the fly-by line using a combination of visual navigation, onboard inertial navigation, and callouts from the control room.

Climb-To-Cruise Tests

The flight matrix for the CTC runs consisted of level flight accelerations over the acoustic array at various Mach numbers and altitudes. During these runs, the engine power setting was constant at 85° (intermediate) in order to obtain the maximum engine NPR. Table 1 lists the CTC desired test conditions. Test altitudes desired varied from an altitude of 3,800–32,300 ft, and the Mach numbers ranged from 0.30 to 0.90.

Table 1. Climb-to-cruise test points.

| Mach number | Altitude, ft |
|-------------|--------------|
| 0.3 | 3,800 |
| 0.6 | 7,300 |
| 0.65 | 12,300 |
| 0.75 | 22,300 |
| 0.9 | 32,300 |

For the CTC condition, the pilot first stabilized the aircraft at the desired altitude and just below the desired Mach number. As the airplane approached the acoustic start point, based on a radio call from the control room, the throttle was advanced to the intermediate power setting. Then the engine was allowed to stabilize for approximately 5 sec before the start of the test run. The aircraft would accelerate depending on the degree of excess thrust through the desired test conditions in level flight. Some acoustic runs were initiated directly over the center of the array with the run terminating when the elevation angle was again 15° above the horizon. At some flight test conditions, the aircraft speed brakes were deployed to reduce the acceleration during the acoustic data acquisition. Because of aircraft acceleration no data were obtained at the 22,300 and 32,300 ft altitudes for the F-16XL, ship 2, tests.

ANOPP Tests

The ANOPP code evaluation tests were flown at constant Mach number and at an altitude of 3800 ft (1500 ft above the local ground level). Test Mach numbers ranged from 0.30 to 0.95 (table 2). For the ANOPP tests, the throttle setting was the power level flight (PLF) at constant speed and varied from about 35° to 57°. For these runs, the pilot was vectored over the microphone array in similar fashion to the CTC tests. Once power was set, it was not changed during the flyover, so small changes in Mach number occurred. Speed brakes were not used for ANOPP tests.

Table 2. ANOPP test points.

| Mach number | Altitude, ft | Power setting, deg |
|-------------|--------------|--------------------|
| 0.3 | 3800 | ~ 48° |
| 0.6 | 3800 | ~ 35° |
| 0.8 | 3800 | ~ 47° |
| 0.95 | 3800 | ~ 56° |

Table 3 shows the CTC and ANOPP tests that were flown during three flights. Note that all of the CTC tests resulted in a significant change in Mach number during the run, which was caused by the

excess thrust. Repeat tests were flown at some conditions. The data shown with table run letters were the primary acoustics tests for CTC and ANOPP tests. Exhaust flow properties from these tests are shown in table 4.

Table 3. Acoustics flight tests for the F-16XL, ship 2.

| Test for table in this report | Mach number start–end | Altitude, ft | Run legs, mi | Run type |
|----------------------------------|--------------------------|-----------------|-----------------|-------------|
| Flight 1 | | | | |
| A | 0.33–0.75 | ~3,800 | ±2 | CTC |
| B | 0.58–0.95 | ~7,300 | ±4 | CTC |
| C | 0.70–0.92 | ~12,300 | ±7 | CTC |
| D | 0.31–0.79 | ~3,800 | ±2 | CTC |
| Flight 2 | | | | |
| | 0.31–0.61 | ~3,800 | ±2 | CTC |
| | 0.34–0.55 | ~3,800 | ±2 | CTC |
| | 0.31–0.48 | ~3,800 | 0 to –2 | CTC |
| | 0.32–0.47 | ~3,800 | 0 to –2 | CTC |
| | 0.60–0.73 | ~7,300 | ±4 | CTC |
| Flight 3 | | | | |
| | 0.33–0.33 | ~3,800 | ±2 | ANOPP |
| E | 0.31–0.28 | ~3,800 | ±2 | ANOPP |
| | 0.61–0.58 | ~3,800 | ±2 | ANOPP |
| F | 0.60–0.60 | ~3,800 | ±2 | ANOPP |
| G | 0.80–0.81 | ~3,800 | ±2 | ANOPP |
| | 0.80–0.80 | ~3,800 | ±2 | ANOPP |
| H | 0.95–0.95 | ~3,800 | ±2 | ANOPP |
| | 0.94–0.95 | ~3,800 | ±2 | ANOPP |
| | 0.30–0.58 | ~3,800 | ±2 | CTC |
| | 0.28–0.59 | ~3,800 | ±2 | CTC |
| | 0.28–0.49 | ~3,800 | ±2 | CTC |
| | 0.31–0.50 | ~3,800 | 0 to 2 | CTC |

Static Tests

For the static tests, the F-16XL, ship 2, aircraft was tied down, and engine power setting was varied to achieve engine pressure ratio increments of 0.1 from idle to intermediate power (98.5 percent N_2) and then back to idle. At each test point, the engine was allowed to stabilize for 1 min; then acoustic data were acquired for 30 sec. These tests were conducted with the wind speed below 5 kn to minimize wind noise. Atmospheric data were obtained from the NASA Dryden acoustics van and from the Air Force Flight Test Center (AFFTC), Edwards, California, observations.

ANALYTICAL TECHNIQUES

Engine Exhaust Flow Properties

Jet-mixing and shock cell noise are two primary sources of noise for high-NPR engines during take-off and subsonic climb (ref. 2). These noise sources are primarily affected by the aircraft velocity,

exhaust-exit Mach number and velocity, and NPR. For acoustic analysis, exhaust characteristics are often defined at the nozzle exit (station 9) and also at an assumed fully expanded condition (station *jet*) (fig. 3). Jet-mixing noise is primarily a function of the difference between the fully expanded nozzle jet velocity, V_{jet} , and the free stream velocity. Shock cell noise is a function of the difference between the fully expanded jet Mach number, M_{jet} , and the nozzle exit Mach number based on nozzle expansion ratio, M_9 . At the point where $M_9 = M_{jet}$, the shock cell noise is diminished. Nozzle exit velocity from nozzle exit, V_9 , and Mach number M_9 are based on the aerothermodynamic characteristics of the flow at the nozzle exit plane (fig. 3).

F110-GE-129 Digital Engine Model

Flight and ground test data from the instrumented engine did not directly measure values of pressure, temperature, velocity, and mass flow at station 9. At station *jet*, these data did not provide the data needed for the evaluation of CTC and ANOPP codes. A digital engine performance model[†] was used to calculate some of the needed parameters. Others were computed using follow-on calculations.

Engine Model Description

The F110-GE-129 engine performance model (also referred to as the engine deck) is a digital computer FORTRAN program which predicts engine parameters and performance consistent with a nominal F110-GE-129 engine. The aerothermodynamic model calculates the various engine operating parameters. Many of these parameters would otherwise be difficult or impossible to measure because of the excessively high temperatures, inaccessibility of the area to instrumentation, or both.

Data Selection Procedure

Plots of selected flight parameters were compared with the times associated with the pilot call outs for the selected inbound distance, the overhead point, and the selected outbound distance. Results revealed that Mach number, altitude, A_8 , and PLA were the main parameters defining the quality of the data for a test run. A PLA and A_8 , which were constant along with a constant or slowly accelerating Mach number and a relatively constant altitude were needed. In the flight data tables, there are typically three data points per flyover: one at the start point, one at the overhead point, and one at the end point.

Engine Model Inputs

The F110-GE-129 engine deck input parameters used for the analysis consist of altitude, Mach number, T_I , and PLA. The aircraft total temperature probe was inoperative for the acoustics flights, and it was planned to use the T_I . For verification, the engine deck-calculated ambient temperature was compared with the temperature measured by the AFFTC weather balloon at approximately the time of flights 1 and 3. Figure 7 compares the ambient temperatures calculated from the flight T_I measurement with the weather balloon-measured data as a function of altitude. Standard day T_I is shown for reference. The flight and balloon comparisons match well enough to justify the use of T_I in combination with aircraft-calculated Mach number and altitude.

[†]Wills, T. K., Cycle Deck User's Manual for F110-GE-129 Performance, GE R89AEB216, May 1989. (Contact General Electric Company, Lynn, Massachusetts.)

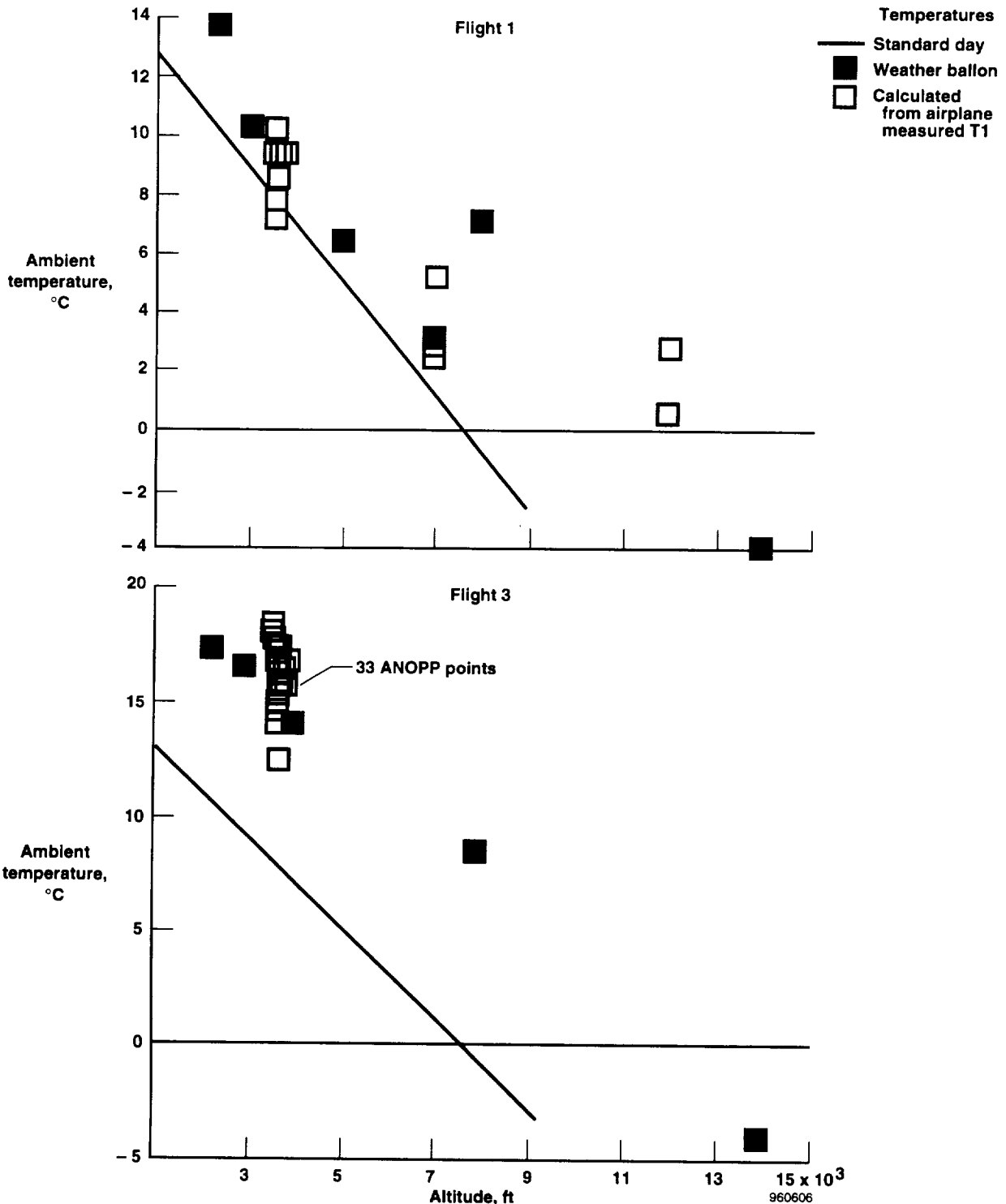


Figure 7. Ambient temperature and standard day temperature for the acoustics flyover tests.

The engine deck uses Mach number and ambient pressure based on altitude to compute the free stream total pressure. The inlet pressure recovery curve for the F-16XL, ship 2 (fig. 2(b)), was input into the engine deck to provide the correct engine face pressure recovery.

Engine Model Output

The engine deck, models the engine as a gas generator and predicts output flight parameters based on the measured airplane flight parameters which were previously input. Some of the unmeasurable parameters that were calculated by the engine deck and were needed for the acoustic analysis were gross thrust (F_g); V_{jet} ; NPR; ratio of exhaust nozzle effective exit-plane area to its effective throat area, AE_9/AE_8 ; ratio of exhaust nozzle flow exit-plane static pressure to ambient static pressure, P_{s9}/P_{amb} ; exhaust nozzle mixed-jet total temperature at the throat, T_8 ; mass flow rate at the exhaust nozzle throat, W_8 ; and other useful exhaust nozzle exit stream parameters, such as throat total pressure, P_8 and the specific heat ratio of exhaust gas at nozzle entrance, GAM7. The engine deck also calculates parameters, such as $PT_{2.5}$, P_{s3} , WFE , $N1$, $N2$, and A_8 which may be compared to the engine measurements.

In addition to the engine deck-calculated value of V_{jet} , the local values of V_9 , M_9 , and M_{jet} were determined from later calculations.

Exhaust Flow Properties

For these calculations, steady, one-dimensional, adiabatic, isentropic flow was assumed to exist between the planes of the nozzle inlet (station 7) and the nozzle exit (station 9). One of three possible cases is assumed to exist at the nozzle exit plane depending on the level of static pressure (P_{s9}) existing at the moment of data sampling. If the condition ($P_{s9} < P_{amb}$) exists, the flow is said to be overexpanded. If the condition ($P_{s9} = P_{amb}$) exists, the flow is said to be fully expanded. When the condition ($P_{s9} > P_{amb}$) exists, the flow is said to be underexpanded. In all cases, it is assumed that total temperature and specific heat ratio of exhaust gas is equal at stations 7, 8, 9, and *jet*.

Ideal or Jet Expansion Parameters

One way to calculate exhaust properties is to assume that the total pressure at the nozzle throat is isentropically expanded to atmospheric pressure. These *jet* parameters are independent of the nozzle expansion ratio and are only a function of NPR. The M_{jet} parameter uses this assumption.

Area Ratio Parameters

M_9 is another parameter of interest for acoustic analysis. This parameter is determined based entirely on the ratio of the exhaust nozzle area at the exit plane to its area at the throat, A_9/A_8 . It assumes that the flow expands isentropically from the throat to the exit regardless of what the exit static pressure may be. For the engine deck, an effective area ratio, AE_9/AE_8 is calculated and may be used to calculate M_9 . This calculation is only useful for cases in which the flow at station 8 is choked.

Exhaust Static Temperature

The exhaust nozzle exit and fully expanded *jet* static temperatures, T_{s9} and T_{sjet} , are calculated from T_8 using GAM7 from the engine deck.

Local Speed of Sound and Exhaust Velocities

The speed of sound propagation in the hot gas stream was calculated using conventional gas dynamics relationships, then multiplied by the Mach number to arrive at the exhaust velocities. These calculations were performed in a follow-on program to supplement the engine deck outputs.

RESULTS AND DISCUSSION

The results of the ground run, CTC tests, and ANOPP tests are presented in tables 4, 5, and 6. Each table shows first, in part (a), the measured input data and measured engine parameters; second, in part (b), a comparison of the engine deck-calculated values to the engine measurements; and third, in part (c), the engine deck and follow-on calculated exhaust parameters. For the flyovers, there are usually three data points: one at the beginning of the run, one at the overhead point, and one at the end.

Table 4. F-16XL, ship 2, ground run test.
(a) Measured and engine deck-calculated parameters.

| Mach number 0.0, pressure altitude = 2270 ft | | | | | | | | | | | | |
|--|---------------|----------|---------------------------|-------------|-------------------------|----------------------------|--------------------------|-----------|---------|---------|---------|---------------------|
| Test point | Input to deck | | | Deck output | | Measured engine parameters | | | | | | |
| | PLA, deg | Tamb, °R | Pamb, lbf/in ² | T1, °R | P1, lbf/in ² | PT2.5, lbf/in ² | Ps3, lbf/in ² | WFE, lb/h | N1, rpm | N2, rpm | EGT, °R | A8, in ² |
| 1 | 20.4 | 517.6 | 13.53 | 517.6 | 13.2 | 15.9 | 53 | 1179 | 3141 | 10354 | 1456 | 965 |
| 2 | 24.7 | 517.6 | 13.53 | 517.6 | 13.1 | 17.5 | 71 | 1587 | 3992 | 11126 | 1426 | 770 |
| 3 | 30.5 | 517.6 | 13.53 | 517.6 | 13.0 | 21.0 | 108 | 2513 | 5113 | 11899 | 1445 | 520 |
| 4 | 32.5 | 517.6 | 13.53 | 517.6 | 12.9 | 21.8 | 116 | 2663 | 5341 | 12062 | 1530 | 519 |
| 5 | 38.7 | 517.6 | 13.53 | 517.6 | 12.8 | 24.6 | 145 | 3481 | 6051 | 12529 | 1542 | 496 |
| 6 | 43.9 | 517.6 | 13.53 | 517.6 | 12.6 | 26.5 | 168 | 4062 | 6491 | 12846 | 1580 | 491 |
| 7 | 48.9 | 517.6 | 13.53 | 517.6 | 12.5 | 28.1 | 185 | 4578 | 6858 | 13117 | 1631 | 489 |
| 8 | 55.1 | 517.6 | 13.53 | 517.6 | 12.3 | 30.1 | 207 | 5310 | 7207 | 13445 | 1678 | 492 |
| 9 | 60.2 | 517.6 | 13.53 | 517.6 | 12.1 | 31.7 | 227 | 6042 | 7510 | 13765 | 1732 | 499 |
| 10 | 67.6 | 517.6 | 13.53 | 517.6 | 12.0 | 33.8 | 251 | 6882 | 7693 | 14033 | 1793 | 482 |
| 11 | 72.8 | 517.6 | 13.53 | 517.6 | 11.8 | 36.7 | 287 | 8197 | 7860 | 14339 | 1899 | 444 |
| 12 | 83.6 | 517.6 | 13.53 | 517.6 | 11.4 | 38.5 | 312 | 9427 | 8187 | 14663 | 1999 | 445 |
| 13 | 85.2 | 517.6 | 13.53 | 517.6 | 11.4 | 38.3 | 314 | 9385 | 8215 | 14710 | 1996 | 444 |
| 14 | 53.7 | 517.6 | 13.53 | 517.6 | 12.4 | 29.7 | 205 | 5116 | 7135 | 13414 | 1628 | 488 |
| 15 | 29.7 | 517.6 | 13.53 | 517.6 | 13.0 | 20.4 | 104 | 2276 | 4972 | 11859 | 1379 | 546 |
| 16 | 15.2 | 517.6 | 13.53 | 517.6 | 13.2 | 15.9 | 52 | 1201 | 3111 | 10400 | 1497 | 975 |

Table 4. Continued.
(b) Comparison of measured and engine deck-calculated engine parameters.

| Test point | PLA, deg | PT2.5, lbf/in ² | | Ps3, lbf/in ² | | WFE, lb/h | | N1, rpm | | N2 rpm | | A8, in ² | |
|------------|----------|----------------------------|------|--------------------------|-------|-----------|------|---------|------|--------|-------|---------------------|------|
| | | Meas | Deck | Meas | Deck | Meas | Deck | Meas | Deck | Meas | Deck | Meas | Deck |
| 1 | 20.4 | 15.9 | 16.2 | 52.5 | 50.0 | 1179.1 | 1117 | 3141 | 3105 | 10354 | 10187 | 965 | 958 |
| 2 | 24.7 | 17.5 | 17.8 | 71.3 | 70.7 | 1587.3 | 1434 | 3992 | 3961 | 11126 | 11137 | 770 | 761 |
| 3 | 30.5 | 21.0 | 21.0 | 108.1 | 107.1 | 2512.9 | 2233 | 5113 | 5094 | 11899 | 11950 | 520 | 520 |
| 4 | 32.5 | 21.8 | 21.8 | 115.7 | 115.0 | 2663.4 | 2420 | 5341 | 5253 | 12062 | 12094 | 519 | 520 |
| 5 | 38.7 | 24.6 | 24.7 | 145.3 | 146.0 | 3480.9 | 3227 | 6051 | 6052 | 12529 | 12590 | 496 | 490 |
| 6 | 43.9 | 26.5 | 26.7 | 167.6 | 167.0 | 4061.8 | 3803 | 6491 | 6500 | 12846 | 12858 | 491 | 485 |
| 7 | 48.9 | 28.1 | 28.3 | 184.6 | 184.0 | 4578.1 | 4298 | 6858 | 6872 | 13117 | 13083 | 489 | 485 |
| 8 | 55.1 | 30.1 | 30.5 | 207.1 | 209.0 | 5309.9 | 5049 | 7207 | 7235 | 13445 | 13442 | 492 | 487 |
| 9 | 60.2 | 31.7 | 32.4 | 227.3 | 232.0 | 6041.9 | 5814 | 7510 | 7520 | 13765 | 13733 | 499 | 491 |
| 10 | 67.6 | 33.8 | 34.6 | 251.3 | 260.0 | 6881.9 | 6728 | 7693 | 7740 | 14033 | 14079 | 482 | 477 |
| 11 | 72.8 | 36.7 | 37.0 | 287.3 | 290.0 | 8196.8 | 7760 | 7860 | 7887 | 14339 | 14423 | 444 | 448 |
| 12 | 83.6 | 38.5 | 39.7 | 312.5 | 325.0 | 9427.0 | 9191 | 8187 | 8224 | 14663 | 14696 | 445 | 448 |
| 13 | 85.2 | 38.3 | 39.9 | 313.8 | 327.0 | 9384.8 | 9262 | 8215 | 8241 | 14710 | 14709 | 444 | 449 |

Table 4. Concluded.
(c) Deck output and calculated exhaust parameters.

| Test point | PLA, deg | P8, lbf/in ² | T8, °R | GAM7 | Fg, lbf | W8, lb/sec | AE9/AE8 | Exhaust properties | | | | | |
|------------|----------|-------------------------|--------|-------|---------|------------|---------|---------------------|------------|----------|-------------|-------|--------------|
| | | | | | | | | Station 9, f(A9/A8) | | | Jet, f(NPR) | | |
| | | | | | | | | M9 | V9, ft/sec | Ps9/Pamb | NPR | Mjet | Vjet, ft/sec |
| 1 | 20.4 | 13.8 | 852 | 1.386 | 466 | 67.4 | 1.298 | – | – | – | 1.019 | 0.173 | 232 |
| 2 | 24.7 | 14.2 | 848 | 1.387 | 1028 | 89.1 | 1.261 | – | – | – | 1.053 | 0.279 | 385 |
| 3 | 30.5 | 16.7 | 918 | 1.382 | 2753 | 114.9 | 1.121 | – | – | – | 1.233 | 0.561 | 800 |
| 4 | 32.5 | 17.1 | 929 | 1.381 | 3079 | 121.2 | 1.121 | – | – | – | 1.263 | 0.594 | 849 |
| 5 | 38.7 | 19.4 | 991 | 1.377 | 4537 | 140.2 | 1.100 | 1.372 | 1804.1 | 0.47 | 1.436 | 0.746 | 1082 |
| 6 | 43.9 | 21.0 | 1032 | 1.374 | 5498 | 151.9 | 1.096 | 1.362 | 1831.0 | 0.52 | 1.550 | 0.826 | 1210 |
| 7 | 48.9 | 22.2 | 1065 | 1.372 | 6302 | 161.3 | 1.096 | 1.362 | 1859.3 | 0.55 | 1.642 | 0.882 | 1302 |
| 8 | 55.1 | 24.0 | 1115 | 1.368 | 7426 | 173.2 | 1.097 | 1.364 | 1904.7 | 0.59 | 1.770 | 0.952 | 1423 |
| 9 | 60.2 | 25.6 | 1165 | 1.364 | 8478 | 153.6 | 1.100 | 1.368 | 1950.9 | 0.63 | 1.890 | 1.011 | 1529 |
| 10 | 67.6 | 28.2 | 1233 | 1.359 | 9732 | 191.5 | 1.090 | 1.348 | 1984.8 | 0.72 | 2.088 | 1.095 | 1682 |
| 11 | 72.8 | 31.9 | 1321 | 1.353 | 11049 | 195.3 | 1.068 | 1.300 | 1998.4 | 0.87 | 2.360 | 1.194 | 1867 |
| 12 | 83.6 | 34.6 | 1411 | 1.347 | 12626 | 206.8 | 1.070 | 1.305 | 2070.6 | 0.94 | 2.559 | 1.258 | 2009 |
| 13 | 85.2 | 34.7 | 1415 | 1.346 | 12696 | 207.3 | 1.071 | 1.307 | 2076.4 | 0.94 | 2.567 | 1.261 | 2015 |
| 14 | 53.7 | 23.5 | 1101 | 1.369 | 7133 | 170.2 | 1.097 | 1.360 | 1888.8 | 0.58 | 1.737 | 0.935 | 1392 |
| 15 | 29.7 | 16.3 | 906 | 1.383 | 2503 | 111.7 | 1.132 | – | – | – | 1.203 | 0.527 | 748 |
| 16 | 15.2 | 13.8 | 852 | 1.386 | 457 | 67.5 | 1.300 | – | – | – | 1.018 | 0.170 | 227 |

Table 5. CTC test data.
(a) CTC measured and input to deck data.

| | | Measured and calculated inputs to deck | | | | Calculated by deck | | | | Measured engine data | | | | | |
|--------------|-------|---|----------------|-----------------|-----------|--------------------|------------------------------|----------------------------|-------------------------------|-----------------------------|--------------|------------|------------|------------|------------------------|
| Test Segment | | PLA, deg | Mach number | Altitude, ft | T1, °R | Tamb, °R | Pamb, lbf/in ² | P1, lbf/in ² | PT2.5, lbf/in ² | Ps3, lbf/in ² | WFE, lb/h | N1, rpm | N2, rpm | EGT, °R | A8, in ² |
| A | Start | 85.0 | 0.344 | 3565 | 520.9 | 508.9 | 12.90 | 13.72 | 45.6 | 381 | 10789 | 8305 | 14686 | 1846 | 446 |
| A | OH | 85.0 | 0.557 | 3610 | 538.5 | 507.1 | 12.88 | 15.58 | 53.2 | 440 | 12911 | 8470 | 14936 | 2153 | 446 |
| A | End | 85.0 | 0.758 | 3603 | 563.4 | 505.3 | 12.89 | 18.47 | 61.8 | 500 | 14654 | 8536 | 15060 | 2027 | 447 |
| B | Start | 85.1 | 0.622 | 7042 | 540.1 | 501.3 | 11.32 | 14.18 | 49.3 | 410 | 12071 | 8470 | 14887 | 1920 | 446 |
| B | OH | 85.0 | 0.852 | 7040 | 569.6 | 497.4 | 11.32 | 17.83 | 58.9 | 477 | 13869 | 8547 | 15044 | 2156 | 447 |
| B | End | 85.0 | 0.945 | 7035 | 585.5 | 496.8 | 11.33 | 19.73 | 63.1 | 501 | 14853 | 8566 | 15029 | 2190 | 447 |
| C | OH | 85.0 | 0.684 | 11975 | 543.4 | 496.9 | 09.36 | 12.54 | 42.6 | 356 | 10724 | 8486 | 14866 | 1998 | 445 |
| C | End | 85.0 | 0.946 | 12060 | 581.3 | 493.1 | 09.32 | 16.26 | 52.5 | 422 | 12442 | 8556 | 15044 | 2160 | 447 |
| D | Start | 85.1 | 0.329 | 3498 | 521.3 | 510.3 | 12.93 | 13.66 | 44.9 | 376 | 11033 | 8300 | 14607 | 1821 | 446 |
| D | OH | 85.1 | 0.563 | 3540 | 541.6 | 509.3 | 12.91 | 15.69 | 53.7 | 447 | 13005 | 8492 | 14960 | 2130 | 446 |
| D | End | 85.1 | 0.755 | 3558 | 563.6 | 486.1 | 12.90 | 18.45 | 61.4 | 499 | 12957 | 8520 | 15094 | 2136 | 446 |

Table 5. Continued.
(b) Comparison of measured and deck-calculated engine parameters.

| | | PLA, deg | Mach number | PT2.5, lbf/in ² | | Ps3, lbf/in ² | | WFE, lb/h | | N1, rpm | | N2, rpm | | A8, in ² | |
|--------------|-------|-------------|----------------|-------------------------------|------|-----------------------------|------|--------------|-------|------------|------|------------|-------|------------------------|------|
| Test Segment | | | | Meas | Deck | Meas | Deck | Meas | Deck | Meas | Deck | Meas | Deck | Meas | Deck |
| A | Start | 85.0 | 0.344 | 45.6 | 47.9 | 381 | 395 | 10789 | 11099 | 8305 | 8295 | 14686 | 14775 | 446 | 450 |
| A | OH | 85.0 | 0.557 | 53.2 | 55.0 | 440 | 456 | 12911 | 13161 | 8470 | 8469 | 14936 | 15034 | 446 | 451 |
| A | End | 85.0 | 0.758 | 61.8 | 63.0 | 500 | 511 | 14654 | 14797 | 8536 | 8535 | 15060 | 15098 | 447 | 452 |
| B | Start | 85.1 | 0.622 | 49.3 | 50.9 | 410 | 420 | 12071 | 12173 | 8470 | 8476 | 14887 | 15049 | 446 | 450 |
| B | OH | 85.0 | 0.852 | 58.9 | 59.9 | 477 | 482 | 13869 | 13834 | 8547 | 8542 | 15044 | 15039 | 447 | 452 |
| B | End | 85.0 | 0.945 | 63.1 | 64.2 | 501 | 508 | 14853 | 14609 | 8566 | 8561 | 15029 | 15078 | 447 | 452 |
| C | OH | 85.0 | 0.684 | 42.6 | 44.1 | 356 | 392 | 10724 | 10577 | 8486 | 8490 | 14866 | 15066 | 445 | 450 |
| C | End | 85.0 | 0.946 | 52.5 | 53.7 | 422 | 456 | 12442 | 12357 | 8556 | 8556 | 15044 | 15074 | 447 | 447 |
| D | Start | 85.1 | 0.329 | 44.9 | 47.6 | 376 | 392 | 11033 | 11020 | 8300 | 8287 | 14607 | 14772 | 446 | 449 |
| D | OH | 85.1 | 0.563 | 53.7 | 55.3 | 447 | 456 | 13005 | 13208 | 8492 | 8482 | 14960 | 15057 | 446 | 451 |
| D | End | 85.1 | 0.755 | 61.4 | 64.4 | 499 | 529 | 14700 | 15215 | 8520 | 8482 | 15094 | 15009 | 446 | 452 |

Table 5. Concluded.
(c) CTC deck and calculated parameters.

| Test | Segment | PLA, deg | Mach number | P8, lbf/in ² | T8, °R | GAM7 | W8, lb/sec | Fg, lb | AE9/ AE8 | Exhaust characteristics | | | | | |
|------|---------|-------------|----------------|----------------------------|-----------|-------|---------------|-----------|-------------|-------------------------|---------------|--------------|-------------|-----------------|------|
| | | | | | | | | | | Station 9, f(AE9/AE8) | | | Jet, f(NPR) | | |
| | | | | | | | | | | M9 | V9, ft/sec | Ps9/ Pamb | NPR | Vjet, ft/sec | Mjet |
| A | Start | 85.0 | 0.344 | 41.8 | 1422 | 1.346 | 248.5 | 16793 | 1.199 | 1.520 | 2328 | 0.88 | 3.24 | 1.428 | 2223 |
| A | OH | 85.0 | 0.557 | 48.2 | 1480 | 1.342 | 280.5 | 20401 | 1.224 | 1.553 | 2412 | 0.96 | 3.74 | 1.528 | 2382 |
| A | End | 85.0 | 0.758 | 54.4 | 1488 | 1.342 | 319.3 | 24189 | 1.224 | 1.553 | 2419 | 1.09 | 4.22 | 1.610 | 2478 |
| B | Start | 85.1 | 0.622 | 44.5 | 1484 | 1.342 | 258.7 | 19145 | 1.223 | 1.553 | 2415 | 1.01 | 3.93 | 1.562 | 2422 |
| B | OH | 85.0 | 0.852 | 51.2 | 1481 | 1.343 | 304.2 | 23416 | 1.224 | 1.553 | 2413 | 1.17 | 4.52 | 1.656 | 2519 |
| B | End | 85.0 | 0.945 | 54.4 | 1484 | 1.342 | 325.2 | 25462 | 1.224 | 1.553 | 2416 | 1.24 | 4.80 | 1.696 | 2562 |
| C | OH | 85.0 | 0.684 | 38.5 | 1489 | 1.342 | 224.2 | 16852 | 1.223 | 1.552 | 2418 | 1.06 | 4.11 | 1.593 | 2460 |
| C | End | 85.0 | 0.946 | 46.0 | 1496 | 1.342 | 269.9 | 21343 | 1.221 | 1.549 | 2421 | 1.28 | 4.93 | 1.713 | 2590 |
| D | Start | 85.1 | 0.329 | 41.6 | 1421 | 1.346 | 247.1 | 16647 | 1.194 | 1.510 | 2317 | 0.88 | 3.22 | 1.423 | 2216 |
| D | OH | 85.1 | 0.563 | 48.3 | 1493 | 1.342 | 281.2 | 20488 | 1.224 | 1.553 | 2423 | 0.97 | 3.74 | 1.529 | 2386 |
| D | End | 85.1 | 0.755 | 55.7 | 1466 | 1.343 | 330.8 | 25016 | 1.224 | 1.553 | 2401 | 1.11 | 4.32 | 1.625 | 2474 |

Table 6. ANOPP flyover test data.
(a) ANOPP flyover measured input data to deck.

| Test | Segment | Engine data | | | | | | | | | | | | | |
|------|---------|---|----------------|-----------------|-----------|--------------------|------------------------------|----------------------------|-------------------------------|-----------------------------|--------------|------------|------------|------------|------------------------|
| | | Measured and calculated inputs to deck | | | | Calculated by deck | | | | Measured engine parameters | | | | | |
| | | PLA deg | Mach number | Altitude, ft | TI, °R | Tamb, °R | Pamb, lbf/in ² | PI, lbf/in ² | PT2.5, lbf/in ² | Ps3, lbf/in ² | WFE, lb/h | NI, rpm | N2, rpm | EGT, °R | A8, in ² |
| E | Start | 48.5 | 0.308 | 3783 | 530.0 | 520.1 | 12.79 | 13.40 | 30.3 | 201.1 | 4736 | 6948 | 13314 | 1620 | 478 |
| E | OH | 48.5 | 0.300 | 3730 | 530.3 | 520.9 | 12.82 | 13.37 | 30.1 | 200.0 | 5285 | 6936 | 13304 | 1608 | 480 |
| E | End | 48.5 | 0.282 | 3648 | 529.1 | 520.8 | 12.86 | 13.31 | 29.9 | 198.5 | 4619 | 6937 | 13290 | 1607 | 478 |
| F | Start | 35.1 | 0.603 | 3780 | 558.6 | 520.7 | 12.80 | 16.03 | 31.8 | 194.2 | 4360 | 6396 | 13321 | 1576 | 463 |
| F | OH | 35.1 | 0.601 | 3740 | 559.0 | 521.3 | 12.82 | 16.03 | 31.8 | 193.8 | 4332 | 6388 | 13316 | 1579 | 463 |
| F | End | 34.8 | 0.605 | 3750 | 561.3 | 523.0 | 12.81 | 16.08 | 31.8 | 194.0 | 4332 | 6381 | 13318 | 1565 | 459 |
| G | Start | 46.6 | 0.793 | 3728 | 584.5 | 519.2 | 12.82 | 19.02 | 43.5 | 289.3 | 7148 | 7317 | 14069 | 1741 | 469 |
| G | OH | 46.6 | 0.804 | 3735 | 586.5 | 519.4 | 12.82 | 19.23 | 43.8 | 291.1 | 7221 | 7306 | 14064 | 1741 | 469 |
| G | End | 46.6 | 0.814 | 3770 | 589.1 | 520.2 | 12.80 | 19.39 | 43.8 | 293.2 | 7185 | 7308 | 14079 | 1757 | 468 |
| H | Start | 55.5 | 0.946 | 3753 | 610.9 | 518.2 | 12.81 | 22.34 | 54.8 | 379.8 | 9992 | 7815 | 14576 | 1882 | 471 |
| H | OH | 55.6 | 0.955 | 3745 | 611.8 | 517.5 | 12.81 | 22.57 | 55.3 | 382.0 | 9864 | 7823 | 14590 | 1747 | 474 |
| H | End | 55.5 | 0.947 | 3742 | 611.8 | 518.8 | 12.82 | 22.37 | 54.8 | 379.5 | 9864 | 7806 | 14576 | 1719 | 472 |

Table 6. Continued.
(b) Comparison of measured and deck-calculated parameters.

| Test | Segment | PLA, deg | Mach number | $PT_{2.5}$, lbf/in ² | | Ps_3 , lbf/in ² | | WFE , lb/h | | $N1$, rpm | | $N2$, rpm | | $A8$, in ² | |
|------|---------|-------------|----------------|-------------------------------------|------|---------------------------------|-------|-----------------|------|---------------|------|---------------|-------|---------------------------|------|
| | | | | Meas | Deck | Meas | Deck | Meas | Deck | Meas | Deck | Meas | Deck | Meas | Deck |
| E | Start | 48.5 | 0.308 | 30.3 | 30.0 | 201.1 | 195.4 | 4736 | 4506 | 6948 | 6927 | 13314 | 13219 | 478 | 476 |
| E | OH | 48.5 | 0.300 | 30.1 | 30.0 | 200.0 | 195.0 | 5285 | 4497 | 6936 | 6926 | 13304 | 13221 | 480 | 476 |
| E | End | 48.5 | 0.282 | 29.9 | 29.9 | 198.5 | 194.1 | 4619 | 4472 | 6937 | 6918 | 13290 | 13206 | 478 | 476 |
| F | Start | 35.1 | 0.603 | 31.8 | 31.9 | 194.2 | 190.0 | 4360 | 4229 | 6396 | 6344 | 13321 | 13101 | 463 | 458 |
| F | OH | 35.1 | 0.601 | 31.8 | 31.9 | 193.8 | 190.0 | 4332 | 4227 | 6388 | 6345 | 13316 | 13104 | 463 | 458 |
| F | End | 34.8 | 0.605 | 31.8 | 31.7 | 194.0 | 188.0 | 4332 | 4182 | 6381 | 6319 | 13318 | 13103 | 459 | 458 |
| G | Start | 46.6 | 0.793 | 43.5 | 43.8 | 289.3 | 288.0 | 7148 | 6922 | 7317 | 7288 | 14069 | 13895 | 469 | 458 |
| G | OH | 46.6 | 0.804 | 43.8 | 44.2 | 291.1 | 290.0 | 7221 | 6981 | 7306 | 7290 | 14064 | 13911 | 469 | 457 |
| G | End | 46.6 | 0.814 | 43.8 | 44.5 | 293.2 | 291.0 | 7185 | 7022 | 7308 | 7292 | 14079 | 13932 | 468 | 456 |
| H | Start | 55.5 | 0.946 | 54.8 | 55.3 | 379.8 | 381.0 | 9992 | 9722 | 7815 | 7803 | 14576 | 14490 | 471 | 467 |
| H | OH | 55.6 | 0.955 | 55.3 | 55.9 | 382.0 | 385.0 | 9864 | 9834 | 7823 | 7809 | 14590 | 14497 | 474 | 468 |
| H | End | 55.5 | 0.947 | 54.8 | 55.3 | 379.5 | 381.0 | 9864 | 9719 | 7806 | 7804 | 14576 | 14492 | 472 | 467 |

Table 6. Concluded.
(c) ANOPP test engine deck and calculated outputs.

| Test | Segment | PLA, deg | Mach number | P_8 , lbf/in ² | T_8 , °R | GAM7 | F_g , lb | W_8 , lb/sec | $AE9/$ $AE8$ | Exhaust conditions | | | | | |
|------|---------|-------------|----------------|--------------------------------|---------------|-------|---------------|-------------------|-----------------|---------------------------|-------------------|----------------------|-------------|-----------|-----------------------|
| | | | | | | | | | | Station 9, f(AE9/ AE8) | | | Jet, f(NPR) | | |
| | | | | | | | | | | M_9 | V_9 , ft/sec | $Ps_9/$ P_{amb} | NPR | M_{jet} | V_{jet} , ft/sec |
| E | Start | 48.5 | 0.308 | 23.58 | 1078 | 1.371 | 7400 | 170 | 1.089 | 1.35 | 1859 | 0.63 | 1.843 | 0.985 | 1444 |
| E | OH | 48.5 | 0.300 | 23.53 | 1078 | 1.371 | 7363 | 169 | 1.090 | 1.35 | 1859 | 0.63 | 1.836 | 0.981 | 1440 |
| E | End | 48.5 | 0.282 | 23.43 | 1076 | 1.371 | 7288 | 169 | 1.090 | 1.35 | 1857 | 0.62 | 1.822 | 0.975 | 1430 |
| F | Start | 35.1 | 0.603 | 25.14 | 1057 | 1.373 | 7934 | 175 | 1.076 | 1.32 | 1810 | 0.70 | 1.965 | 1.039 | 1496 |
| F | OH | 35.1 | 0.601 | 25.13 | 1058 | 1.373 | 7918 | 175 | 1.076 | 1.32 | 1810 | 0.70 | 1.961 | 1.038 | 1494 |
| F | End | 34.8 | 0.605 | 25.00 | 1058 | 1.373 | 7840 | 174 | 1.076 | 1.32 | 1811 | 0.69 | 1.952 | 1.034 | 1490 |
| G | Start | 46.6 | 0.793 | 34.93 | 1188 | 1.363 | 13499 | 235 | 1.104 | 1.37 | 1973 | 0.91 | 2.724 | 1.298 | 1893 |
| G | OH | 46.6 | 0.804 | 35.24 | 1191 | 1.363 | 13665 | 236 | 1.108 | 1.38 | 1986 | 0.90 | 2.749 | 1.305 | 1902 |
| G | End | 46.6 | 0.814 | 35.46 | 1194 | 1.364 | 13787 | 237 | 1.112 | 1.39 | 1999 | 0.90 | 2.770 | 1.310 | 1911 |
| H | Start | 55.5 | 0.946 | 44.10 | 1290 | 1.356 | 19093 | 290 | 1.237 | 1.53 | 2227 | 0.91 | 3.443 | 1.468 | 2160 |
| H | OH | 55.6 | 0.955 | 44.57 | 1292 | 1.356 | 19373 | 293 | 1.237 | 1.53 | 2229 | 0.92 | 3.478 | 1.475 | 2169 |
| H | End | 55.5 | 0.947 | 44.11 | 1291 | 1.356 | 19091 | 290 | 1.237 | 1.53 | 2228 | 0.91 | 3.442 | 1.468 | 2160 |

Verification of F110-GE-129 Engine Deck

Use of the F110-GE-129 engine deck, which represents a nominal engine, could introduce errors if the flight test engine were significantly different from the assumed nominal engine. To assess such potential errors, a comparison of some engine-measured parameters with calculated parameters from the

engine deck was made. Tables 4(b), 5(b), and 6(b) compare the airplane-measured parameters with the engine deck-calculated parameters. There are six measured engine parameters (in addition to the PLA, Tl , altitude, and Mach number that are inputs to the engine deck) that may be compared with engine deck-calculated parameters. These are $N1$, $N2$, $PT2.5$, $Ps3$, WFE , and $A8$. Inspection of these tables shows very good agreement for these comparisons, indicating that the engine deck is a good representation of the engine flown in the F-16XL, ship 2. Plots of the comparisons are shown in figure 8 for the ground run, figure 9 for the CTC tests, and fig 10 for the ANOPP tests. The ground run, CTC, and ANOPP flyover data show good to excellent agreement between measured and calculated engine parameters.

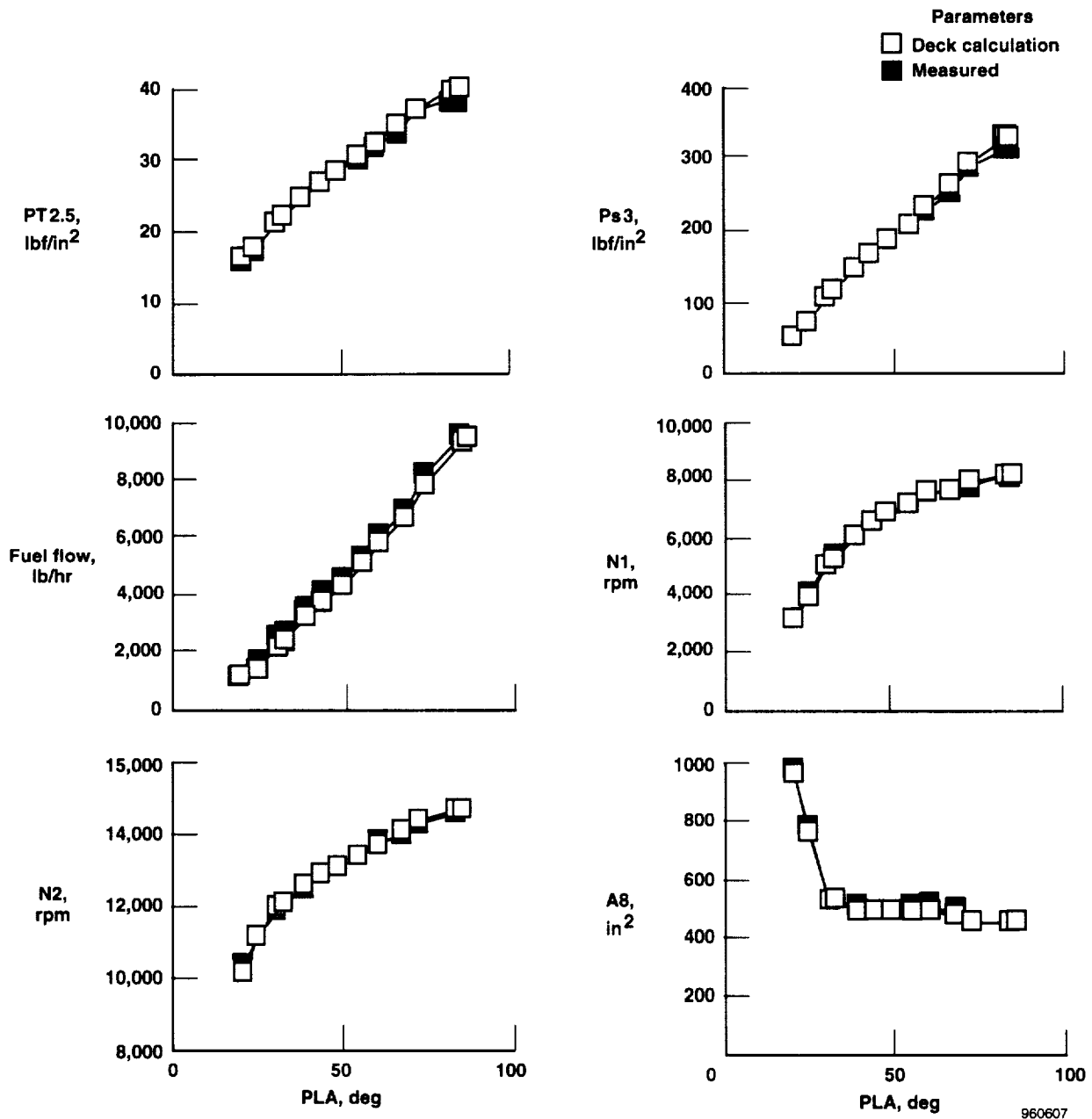


Figure 8. Comparison of measured and deck-calculated parameters, ground run.

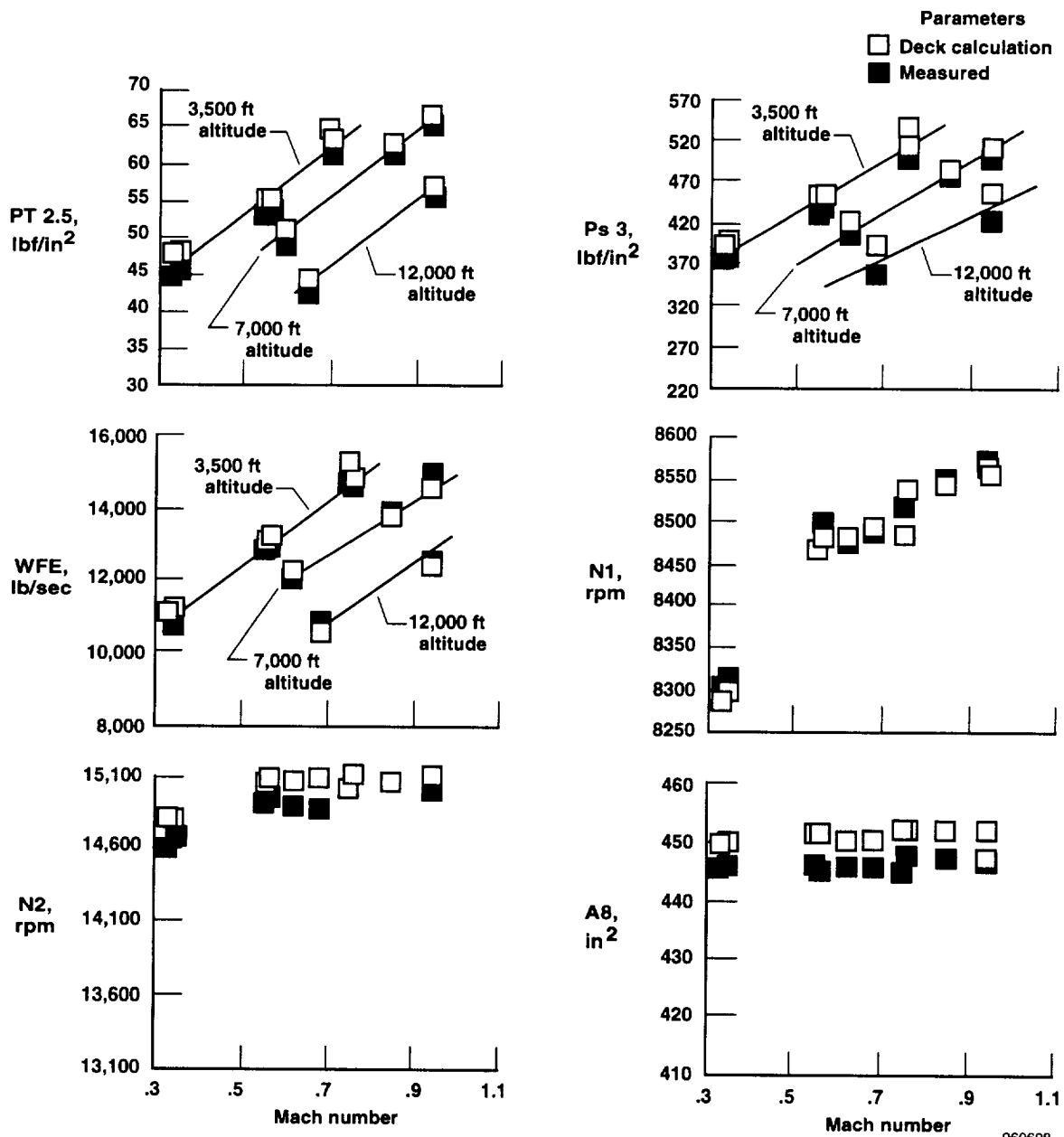


Figure 9. Comparison of measured and deck-calculated parameters, climb-to-cruise tests.

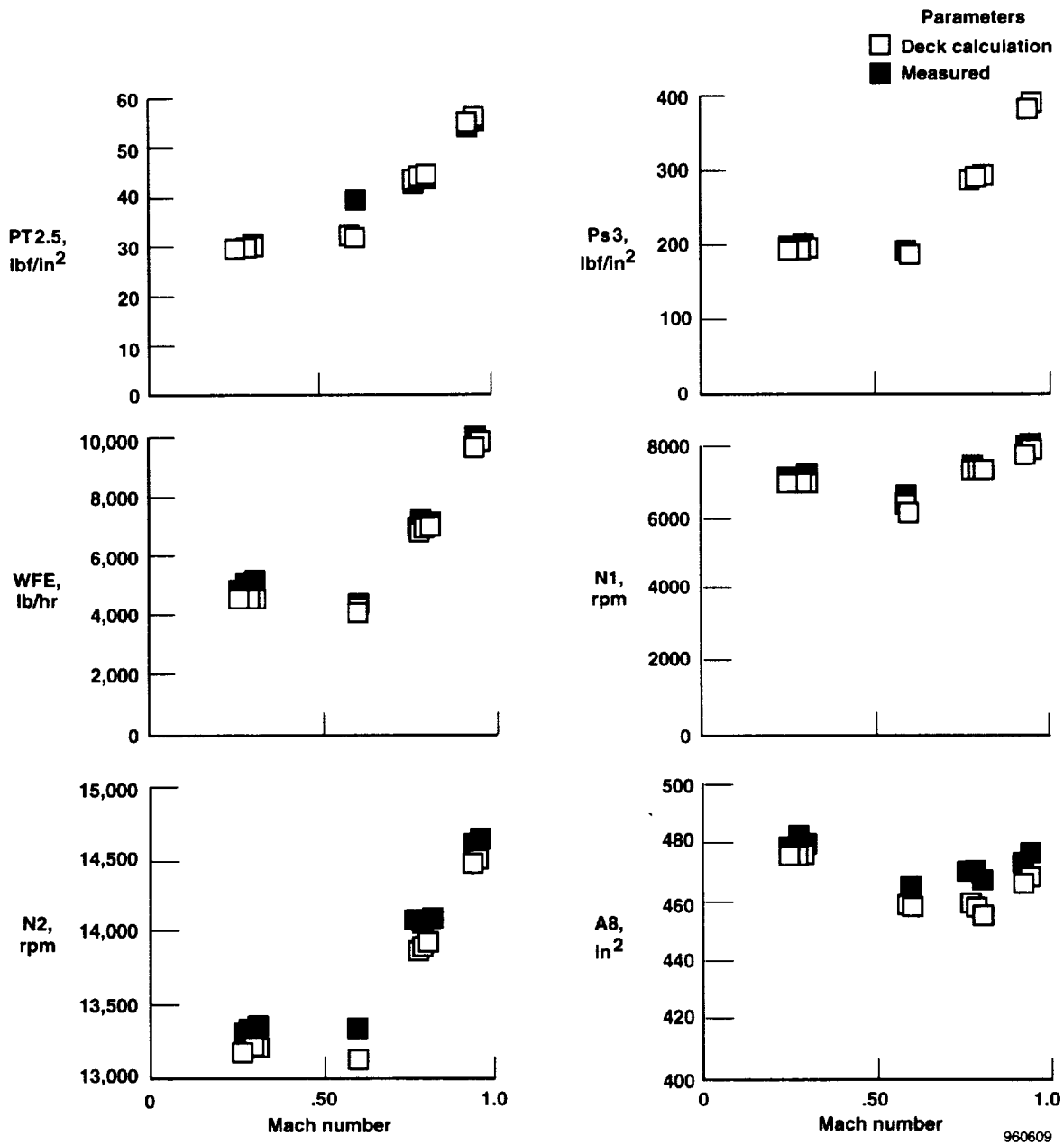


Figure 10. Comparison of measured and deck-calculated parameters, ANOPP tests.

Another indication of the quality of these engine deck data may be inferred from figure 7 which shows temperatures of no more than 10 °C from standard day temperature and not much variation for the 2 test days. Cycle decks tend to be less accurate as deviations from standard day temperature (where much of the cycle deck data were obtained) increase.

Ground Static Test Results

The ground static run data are listed in table 4 for the range of power settings from idle to intermediate. Note that the nozzle is unchoked below a PLA of 38° and is overexpanded for all ground conditions. Maximum NPR is 2.57 at intermediate power.

Figure 11 plots these values for M_{jet} and M_9 versus PLA for the test points where the flow is choked. The M_9 and M_{jet} are separated at the lower values of PLA and approach each other at the higher PLA where the nozzle is only slightly overexpanded. The corresponding values of V_9 and V_{jet} are also plotted showing similar trends to the Mach numbers.

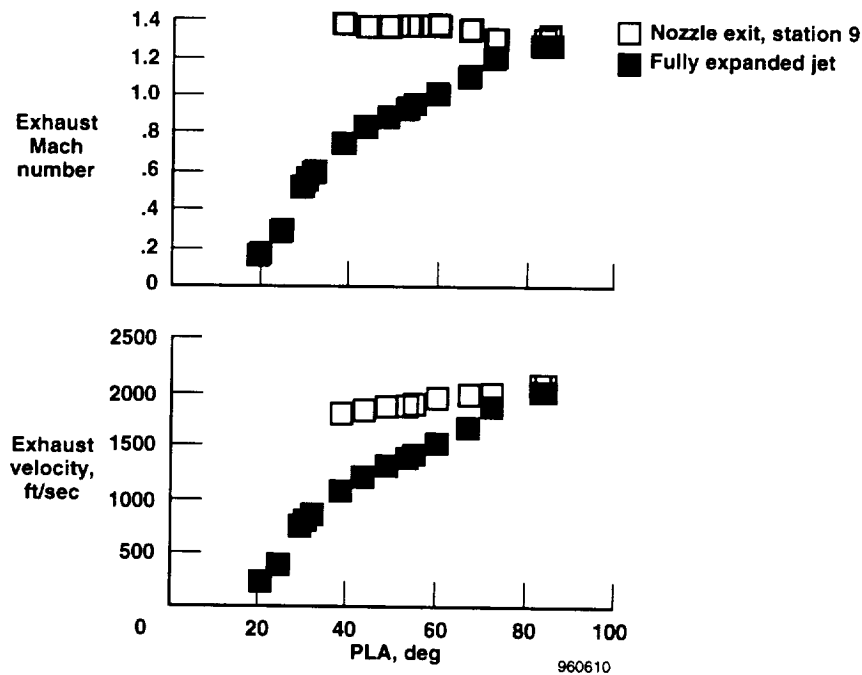


Figure 11. Exhaust flow properties, F110-GE-129 engine in F-16XL, ship 2, ground run.

Flyover Exhaust Flow Properties Results

For most flyover tests, three data points per run are shown: the initial data at the beginning of the run, a point over the microphone array, and the last point at the end of the data run. Table 3 shows a summary of the flyover tests from the three flights. The airplane accelerated rapidly for the CTC tests, while the ANOPP tests were at nearly constant Mach number.

CTC Test Results

Table 5 shows the measured and calculated parameters for the CTC tests. In all cases, the airplane accelerated significantly during the run. Values of NPR varied from 3.2 to almost 5.

Figure 12 shows M_9 and M_{jet} for the CTC conditions and compares both the exhaust Mach numbers and velocities versus the aircraft free stream Mach number. Conditions shown in figure 12 are at intermediate power (PLA = 85°) and at nominal altitudes ranging from 3,800 to 12,300 ft. Because the nozzle area is essentially constant at intermediate power, A_9/A_8 does not vary significantly; therefore, M_9 is almost constant at a value of 1.55. At the lower aircraft Mach numbers (below Mach 0.6), the nozzle flow is overexpanded as it was in the ground run, so $M_{jet} < M_9$. Above Mach 0.6, the nozzle is underexpanded, and $M_{jet} > M_9$. The effects of altitude were quite small as would be expected for V_9 and V_{jet} . Figure 12 shows a similar trend.

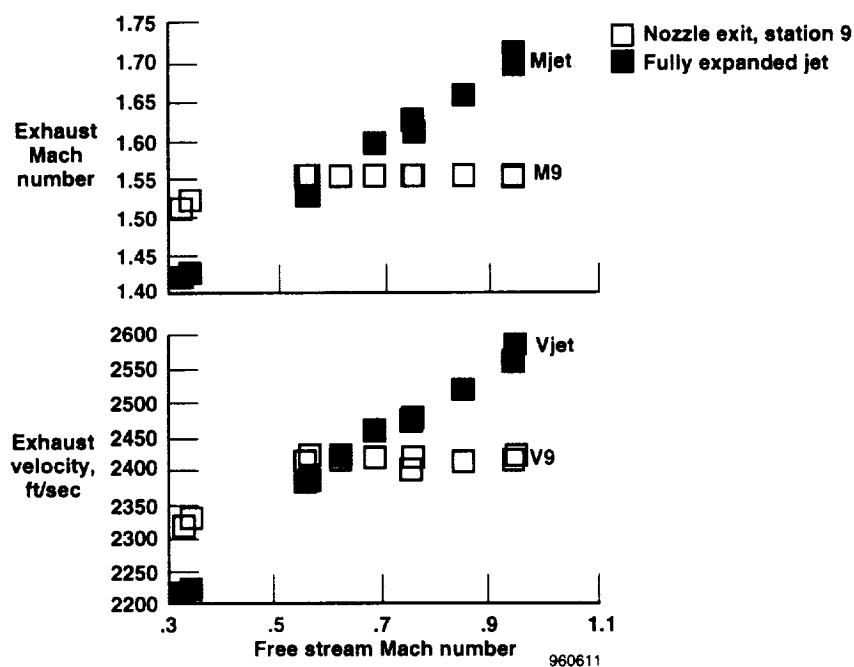


Figure 12. Exhaust flow properties, F110-GE-129 engine in F-16XL, ship 2, climb-to-cruise tests, all tests at intermediate power, for altitudes, see table 5.

ANOPP Test Results

Table 6 lists ANOPP test data from flight 3. The flight points were near an altitude of 3800 ft (1500 ft AGL) and were started two miles before and ended two miles past the microphone array. The PLA was fixed at PLF. Because of the lower power settings, ANOPP test NPR values varied from 1.8 to 3.4. A significant variation also existed in PLA, so the A_9/A_8 parameter varied; hence, M_9 varied from 1.32 to 1.53.

Figure 13 shows the exhaust Mach number and velocity as a function of airplane Mach number. The M_9 is higher than M_{jet} (fig. 13(a)) because the flow is overexpanded at all conditions. Similarly, V_9 is higher than V_{jet} . At the higher Mach number conditions, the nozzle flow is only slightly overexpanded.

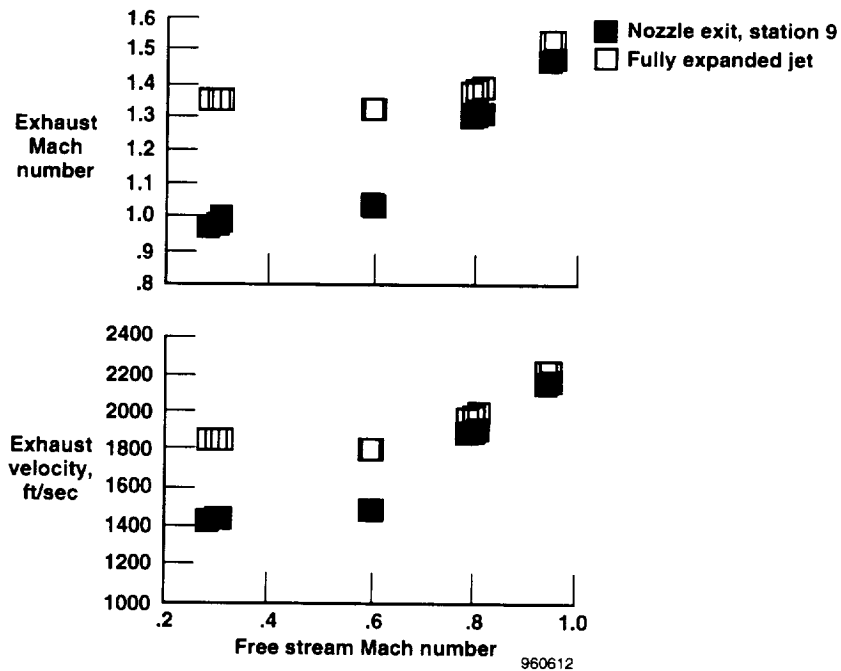


Figure 13. Exhaust flow properties, F110-GE-129 engine in F-16XL, ship 2, ANOPP tests, 3800 ft altitude.

CONCLUDING REMARKS

Flyover and static tests of the F-16XL, ship 2, airplane, powered by the GE F110-GE-129 engine, were conducted as part of a joint NASA Dryden and NASA Langley program to study the acoustics of high nozzle pressure ratio engines. An engine cycle deck was used to calculate parameters for comparison with measured parameters. The engine deck and follow-on calculations were also used to calculate exhaust properties where measurements were not possible. Very good agreement was found between cycle deck-calculated and measured engine parameters. Such agreement gives good confidence in the calculated exhaust properties. Nozzle pressure ratios up to almost 5 occurred at intermediate power, with a maximum jet Mach number of 1.7 and maximum jet velocity of nearly 2600 ft/sec. Nozzle conditions ranged from underexpanded to overexpanded, depending on flight conditions.

*Dryden Flight Research Center
National Aeronautics and Space Administration
Edwards, California, August 1996*

REFERENCES

1. Zorumski, William E., *Aircraft Noise Prediction Program Theoretical Manual*, NASA TM-83199, Part 1, 1982.
2. Ennix, Kimberly A., Burcham, Frank W., and Webb, Lannie D., *Flight-Determined Engine Exhaust Characteristics of an F404 Engine in an F-18 Airplane*, NASA TM-4538, 1993.
3. Ennix, Kimberly A., *Engine Exhaust Characteristics Evaluation in Support of Aircraft Acoustic Testing*, NASA TM-104263, 1993.

REPORT DOCUMENTATION PAGEForm Approved
OMB No. 0704-0188

Public reporting burden for this collection of information is estimated to average 1 hour per response, including the time for reviewing instructions, searching existing data sources, gathering and maintaining the data needed, and completing and reviewing the collection of information. Send comments regarding this burden estimate or any other aspect of this collection of information, including suggestions for reducing this burden, to Washington Headquarters Services, Directorate for Information Operations and Reports, 1215 Jefferson Davis Highway, Suite 1204, Arlington, VA 22202-4302, and to the Office of Management and Budget, Paperwork Reduction Project (0704-0188), Washington, DC 20503.

| | | | |
|--|---|--|---|
| 1. AGENCY USE ONLY (Leave blank) | | 2. REPORT DATE November 1996 | 3. REPORT TYPE AND DATES COVERED Technical Memorandum |
| 4. TITLE AND SUBTITLE Flight and Static Exhaust Flow Properties of an F110-GE-129 Engine in an F-16XL Airplane During Acoustic Tests | | | 5. FUNDING NUMBERS WU 505-68-10 |
| 6. AUTHOR(S) Jon K. Holzman, Lannie D. Webb, and Frank W. Burcham, Jr. | | | |
| 7. PERFORMING ORGANIZATION NAME(S) AND ADDRESS(ES) NASA Dryden Flight Research Center P.O. Box 273 Edwards, California 93523-0273 | | | 8. PERFORMING ORGANIZATION REPORT NUMBER H-2122 |
| 9. SPONSORING/MONITORING AGENCY NAME(S) AND ADDRESS(ES) National Aeronautics and Space Administration Washington, DC 20546-0001 | | | 10. SPONSORING/MONITORING AGENCY REPORT NUMBER NASA TM-104326 |
| 11. SUPPLEMENTARY NOTES | | | |
| 12a. DISTRIBUTION/AVAILABILITY STATEMENT Unclassified—Unlimited Subject Category 07 | | | 12b. DISTRIBUTION CODE |
| 13. ABSTRACT (Maximum 200 words) The exhaust flow properties (mass flow, pressure, temperature, velocity, and Mach number) of the F110-GE-129 engine in an F-16XL airplane were determined from a series of flight tests flown at NASA Dryden Flight Research Center, Edwards, California. These tests were performed in conjunction with NASA Langley Research Center, Hampton, Virginia (LaRC) as part of a study to investigate the acoustic characteristics of jet engines operating at high nozzle pressure conditions. The range of interest for both objectives was from Mach 0.3 to Mach 0.9. NASA Dryden flew the airplane and acquired and analyzed the engine data to determine the exhaust characteristics. NASA Langley collected the flyover acoustic measurements and correlated these results with their current predictive codes. This paper describes the airplane, tests, and methods used to determine the exhaust flow properties and presents the exhaust flow properties. No acoustics results are presented. | | | |
| 14. SUBJECT TERMS Acoustics; F110 engine; F-16XL airplane; Flyover noise | | | 15. NUMBER OF PAGES 32 |
| | | | 16. PRICE CODE A03 |
| 17. SECURITY CLASSIFICATION OF REPORT Unclassified | 18. SECURITY CLASSIFICATION OF THIS PAGE Unclassified | 19. SECURITY CLASSIFICATION OF ABSTRACT Unclassified | 20. LIMITATION OF ABSTRACT Unlimited |